

Cross-correlation between spiral modes and its influence on the overall spatial characteristics of partially coherent beams

R. Martínez-Herrero¹, A. Manjavacas² and P. M. Mejías^{1,*}

¹ Departamento de Óptica, Facultad de Ciencias Físicas,
Universidad Complutense de Madrid, 28040-Madrid, Spain

² Instituto de Óptica, CSIC, Serrano 121, 28006-Madrid, Spain

*pmmejas@fis.ucm.es

Abstract: The overall spatial structure of a general partially coherent field is shown to be connected with the cross-correlation between the so-called spiral modes, understood as the terms of the spiral-harmonics series expansion of the field. The formalism based on the beam irradiance-moments is used, and the light field is globally described by the beam width, the far-field divergence, the beam quality factor, the orientation of the beam profile and the angular orbital momentum, given as the sum of its asymmetrical and vortex parts. This overall spatial description is expressed in terms of the intermodal coherence features (cross-correlation between spiral modes). The above analytical results are also illustrated by means of an example.

©2009 Optical Society of America

OCIS codes: (140.3295) Laser beam characterization; (030.1640) Coherence; (350.5500) Propagation

References and links

1. Y. Liu, C. Gao, M. Gao, and F. Li, "Coherent-mode representation and orbital angular momentum spectrum of partially coherent beam," *Opt. Commun.* **281**, 1968–1975 (2008).
2. R. Martínez-Herrero, and A. Manjavacas, "Overall second-order parametric characterization of light beams propagating through spiral phase elements," *Opt. Commun.* **282**(4), 473–477 (2009).
3. G. Molina-Terriza, J. P. Torres, and L. Torner, "Management of the angular momentum of light: Preparation of photons in multidimensional vector states of angular momentum," *Phys. Rev. Lett.* **88**, 0136011–0136014 (2002).
4. M. V. Vasnetsov, J. P. Torres, D. V. Petrov, and L. Torner, "Observation of the orbital angular momentum spectrum of a light beam," *Opt. Lett.* **28**(23), 2285–2287 (2003).
5. L. Torner, J. P. Torres, and S. Carrasco, "Digital spiral imaging," *Opt. Express* **13**(3), 873–881 (2005).
6. L. Allen, M. W. Beijersbergen, R. J. C. Spreeuw, and J. P. Woerdman, "Orbital angular momentum of light and the transformation of Laguerre-Gaussian laser modes," *Phys. Rev. A* **45**(11), 8185–8189 (1992).
7. L. Allen, M. J. Padgett, and M. Babiker, "The orbital angular momentum of light," *Prog. Opt.* **39**, 291–372 (1999).
8. M. S. Soskin, V. N. Gorshkov, M. V. Vasnetsov, J. T. Malos, and N. R. Heckenberg, "Topological charge and angular momentum of light beams carrying optical vortices," *Phys. Rev. A* **56**(5), 4064–4075 (1997).
9. M. V. Soskin, and M. V. Vasnetsov, "Singular optics," *Prog. Opt.* **42**, 219–276 (2001).
10. H. F. Schouten, G. Gbur, T. D. Visser, and E. Wolf, "Phase singularities of the coherence functions in Young's interference pattern," *Opt. Lett.* **28**(12), 968–970 (2003).
11. T. Alieva, and M. J. Bastiaans, "Evolution of the vortex and the asymmetrical parts of orbital angular momentum in separable first-order optical systems," *Opt. Lett.* **29**(14), 1587–1589 (2004).
12. A. Mair, A. Vaziri, G. Weihs, and A. Zeilinger, "Entanglement of the orbital angular momentum states of photons," *Nature* **412**(6844), 313–316 (2001).
13. G. Gibson, J. Courtial, M. J. Padgett, M. Vasnetsov, V. Pas'ko, S. M. Barnett, and S. Franke-Arnold, "Free-space information transfer using light beams carrying orbital angular momentum," *Opt. Express* **12**(22), 5448–5456 (2004).
14. R. Simon, N. Mukunda, and E. C. G. Sudarshan, "Partially coherent beams and a generalized ABCD-law," *Opt. Commun.* **65**(5), 322–328 (1988).
15. S. Lavi, R. Prochaska, and E. Keren, "Generalized beam parameters and transformation law for partially coherent light," *Appl. Opt.* **27**(17), 3696–3703 (1988).

16. M. J. Bastiaans, "Propagation laws for the second-order moments of the Wigner distribution function in first-order optical systems," *Optik (Stuttg.)* **82**, 173–181 (1989).
17. A. E. Siegman, "New developments in laser resonators" in *Laser Resonators*, Proc. SPIE **1224**, 2–14 (1990).
18. H. Weber, "Propagation of higher-order intensity moments in quadratic-index media," *Opt. Quantum Electron.* **24**(9), S1027–1049 (1992).
19. R. Martínez-Herrero, and P. M. Mejías, "Expansion of the cross-spectral density function of general fields and its application to beam characterization," *Opt. Commun.* **94**(4), 197–202 (1992).
20. R. Martínez-Herrero, P. M. Mejías, G. Piquero, and J. M. Movilla, "Parametric characterization of the spatial structure of non-uniformly polarized laser beams," *Prog. Quantum Electron.* **26**(2), 65–130 (2002).
21. A. Ya. Bekshaev, M. V. Vasnetsov, V. G. Denisenko, and M. S. Soskin, "Transformation of the orbital angular momentum of a beam with optical vortex in an astigmatic optical system," *JETP Lett.* **75**(3), 127–130 (2002).
22. A. Ya Bekshaev, M. S. Soskin, and M. V. Vasnetsov, "Optical vortex symmetry breakdown and decomposition of the orbital angular momentum of light beams," *J. Opt. Soc. Am. A* **20**(8), 1635–1643 (2003).
23. M. J. Bastiaans, "The Wigner distribution function applied to optical signals and systems," *Opt. Commun.* **25**(1), 26–30 (1978).
24. R. Martínez-Herrero, and P. M. Mejías, "On the control of the spatial orientation of the transverse profile of a light beam," *Opt. Express* **14**(3), 1086–1093 (2006).
25. R. Martínez-Herrero, and P. M. Mejías, "On the spatial orientation of the transverse irradiance profile of partially coherent beams," *Opt. Express* **14**(8), 3294–3303 (2006).
26. R. Simon, and N. Mukunda, "Twisted Gaussian-Schell-model beams," *J. Opt. Soc. Am. A* **10**(1), 95–109 (1993).
27. F. Gori, V. Bagini, M. Santarsiero, F. Frezza, G. Schettini, and G. Schirripa Spagnolo, "Coherent and partially coherent twisting beams," *Opt. Rev.* **1**, 143–145 (1994).
28. G. Nemes, and A. E. Siegman, "Measurement of all ten second-order moments of an astigmatic beam by use of rotating simple astigmatic (anamorphic) optics," *J. Opt. Soc. Am. A* **11**(8), 2257–2264 (1994).

1. Introduction

As is well known, the field amplitude $E(r, \theta)$ of a (spatially coherent) beam at a plane transverse to the propagation direction z , can be expanded in terms of spiral harmonics in the form [1,2]

$$E(r, \theta) = \sum_n E_n(r) \exp(in\theta), \quad (1)$$

where r and θ denote the polar coordinates at a transverse plane (say $z = 0$), and $E_n(r) \exp(in\theta)$ represents the so-called n -spiral mode associated to $E(r, \theta)$, with

$$E_n(r) = \frac{1}{2\pi} \int_0^{2\pi} E(r, \theta) \exp(-in\theta) d\theta. \quad (2)$$

When light becomes a partially spatially coherent field, the functions $E(r, \theta)$ and $E_n(r)$ should be considered stochastic processes. Consequently, Eq. (1) and (2) should then be understood in the mean-square sense. Expansion (1) is closely related with the so-called orbital angular momentum (OAM) spectrum, introduced some years ago by Molina-Terriza et al. [3] (see also Refs [4,5].): Note first that the OAM concerns the spatial structure of the phase distribution of the field. In particular, Allen et al [6,7]. showed that the OAM takes the value $l\hbar$ per photon for a beam whose phase term is $\exp(il\theta)$, where l denotes the azimuthal number. The OAM spectrum is then generated by the relative powers of the OAM eigenstates, i.e., of the spiral harmonics with different azimuthal numbers.

Apart from the analytical interest for describing optical vortex beams [8–11], the OAM offers a number of potential applications, such as those related with optical communications (e.g., quantum information processing [12], and high-density data transmission [13]).

In the present work, attention will be focused on the cross-correlation between different spiral modes (i.e., their intermodal coherence features). Since light beams exhibit, in general, complicated and irregular spatial structures, a suitable analytical instrument for their overall description and study is the so-called irradiance-moments formalism [14–20]. In this treatment, the spatial structure of a partially coherent field is globally described (within the paraxial approach) by means of a number of measurable overall parameters. On this basis, it

will be shown in the present work the analytical relationship between the above beam parameters and the intermodal coherence behavior.

The paper will then be arranged as follows. In the next section, the formalism and the key parameters and definitions are introduced. In Section 3, in terms of the cross-correlation between spiral modes, we provide the focusing characteristics at the near- and far-field, the beam quality parameter, the orientation of the beam profile under propagation, and the orbital angular momentum, written as the sum of its asymmetrical and vortex parts [11,21,22]. An illustrative example is discussed in Section 4. Finally, the main conclusions are summarized in Section 5.

2. Basic formalism and key definitions

Let us consider a quasimonochromatic (scalar) partially coherent beam, whose overall spatial behavior is described by means of the beam irradiance moments [14–20] (denoted by sharp brackets). As is well known, they can be defined in terms of the Wigner distribution function [23], $h(\mathbf{r}, \boldsymbol{\eta}, z)$, associated to the field, in the form

$$\langle x^m y^n u^p v^q \rangle \equiv \frac{1}{I} \int x^m y^n u^p v^q h(\mathbf{r}, \boldsymbol{\eta}, z) d\mathbf{r} d\boldsymbol{\eta}, \quad (3)$$

where m, n, p and q are integer numbers, $\mathbf{r} = (x, y)$ is the two-dimensional position vector transverse to the propagation direction z , $k\boldsymbol{\eta} = (ku, kv) = (k_x, k_y)$ provides the wavevector components along the x - and y -axes (u and v would represent angles of propagation, without taking the evanescent waves into account), $I = \int h d\mathbf{r} d\boldsymbol{\eta}$ is proportional to the total beam power, and

$$h(\mathbf{r}, \boldsymbol{\eta}, z) = \int W(\mathbf{r}, \mathbf{s}) \exp(ik\boldsymbol{\eta} \cdot \mathbf{s}) d\mathbf{s}, \quad (4)$$

W being the cross-spectral density (CSD) of the field. Since the four first-order moments, $\langle x \rangle$, $\langle y \rangle$, $\langle u \rangle$ and $\langle v \rangle$, characterize the centre of the beam and its mean direction, in what follows we assume, for simplicity, that these moments vanish. The (squared) beam width at a plane $z = \text{constant}$ and the (squared) far-field divergence are then represented by $\langle x^2 + y^2 \rangle$ and $\langle u^2 + v^2 \rangle$, respectively, and the crossed moment $\langle xu + yv \rangle$ gives the position of the beam waist through the condition $\langle xu + yv \rangle = 0$.

In addition, the spatial orientation of the irradiance profile is characterized [20,24,25] by the orientation of two orthogonal axes (the so-called principal axes) for which the crossed x - y moment vanishes, i.e., $\langle xy \rangle = 0$. It follows that the beam widths $\langle x^2 \rangle^{1/2}$ and $\langle y^2 \rangle^{1/2}$ reach their extreme values along these axes. Since, in general, the spatial profile rotates as the field propagates in free space, the principal axes are useful to describe such rotation. More specifically, the angle α between the principal axes and the laboratory reference axes follows the propagation law [25]

$$\tan 2\alpha(z) = \frac{2 \langle xy \rangle + 2z(\langle xv \rangle + \langle yu \rangle) + 2z^2 \langle uv \rangle}{\langle x^2 \rangle - \langle y^2 \rangle + 2z(\langle xu \rangle - \langle yv \rangle) + z^2(\langle u^2 \rangle - \langle v^2 \rangle)}, \quad (5)$$

z being the propagation distance from the plane where these moments are calculated.

Finally, the orbital angular momentum flux J_z , transported by the beam through a transverse plane $z = \text{constant}$, can be expressed in terms of the irradiance moments in the form [20]

$$J_z = \frac{I}{c} \langle xv - yu \rangle, \quad (6)$$

where c is the speed of light. Note that J_z vanishes for rotationally-symmetric Hermite-Gauss beams, but it differs from zero for twisted Gaussian fields [26–28]. It should be pointed out that the OAM can be decomposed in two parts [21,22], namely, the asymmetrical OAM, denoted by $J_z^{(a)}$ (describing an astigmatic beam with a smooth wavefront), and the vortex OAM, represented by $J_z^{(v)}$ (involving singularities of the wavefront). In terms of the irradiance moments, we have

$$J_z^{(a)} = \frac{I}{c} \left[\frac{1}{\langle x^2 + y^2 \rangle} \left(\langle x^2 - y^2 \rangle \langle xv + yu \rangle + 2 \langle xy \rangle \langle yv - xu \rangle \right) \right], \quad (7.a)$$

and

$$J_z^{(v)} = J_z - J_z^{(a)}. \quad (7.b)$$

Note also that the “beam rotation velocity” $\frac{d\alpha}{dz}$ (where α is given by Eq. (5)) is connected with $J_z^{(a)}$ (cf. Equation (25) of Ref. 22).

All the above second-order parametric characterization can be condensed in the following set of four 2×2 matrices, recently introduced in the literature [25]:

$$\hat{M}^{(0)} = \begin{pmatrix} \langle x^2 + y^2 \rangle & \langle xu + yv \rangle \\ \langle xu + yv \rangle & \langle u^2 + v^2 \rangle \end{pmatrix}, \quad (8.a)$$

$$\hat{M}^{(1)} = \begin{pmatrix} \langle x^2 - y^2 \rangle & \langle xu - yv \rangle \\ \langle xu - yv \rangle & \langle u^2 - v^2 \rangle \end{pmatrix}, \quad (8.b)$$

$$\hat{M}^{(2)} = \begin{pmatrix} 2 \langle xy \rangle & \langle xv + yu \rangle \\ \langle xv + yu \rangle & 2 \langle uv \rangle \end{pmatrix}, \quad (8.c)$$

$$\hat{M}^{(3)} = \begin{pmatrix} 0 & \langle xv - yu \rangle \\ \langle yu - xv \rangle & 0 \end{pmatrix}. \quad (8.d)$$

We see from the definitions that the near- and far-field spatial behavior can be inferred from the diagonal elements of $\hat{M}^{(0)}$. Furthermore, the non-diagonal elements give the position of the waist plane and the determinant of $\hat{M}^{(0)}$ defines the beam quality parameter [20], which provides a joint description of the focusing and collimation capabilities of the light beam.

On the other hand, matrices $\hat{M}^{(1)}$ and $\hat{M}^{(2)}$ include all the second-order parameters required to know the orientation of the beam profile freely propagating as well as the symmetry properties. They also include complete information to determine the asymmetrical OAM. Finally, matrix $\hat{M}^{(3)}$ gives the OAM of the beam: in fact, $\det \hat{M}^{(3)}$ is proportional to $(J_z)^2$.

It should be noted that matrices $\hat{M}^{(i)}$, $i = 0, 1, 2, 3$, propagate through stigmatic optical systems according with the simple law [25]

$$(\hat{M}^{(i)})_{output} = \hat{S} (\hat{M}^{(i)})_{input} \hat{S}^t, \quad (9)$$

where \hat{S} is the 2×2 ABCD matrix representing the system, and t means transposition. Let us finally recall that $\sum_{i=0}^3 \det \hat{M}^{(i)}$ remains invariant upon propagation through general ABCD optical systems [25].

3. Relation between the intermodal coherence and the second-order (overall) spatial characterization

The spiral-mode expansion (1) allows us to express the CSD of the field in the form

$$W(r_1, \theta_1, r_2, \theta_2) = \sum_{n,m} \overline{E_n^*(r_1) E_m(r_2)} \exp(-in\theta_1) \exp(im\theta_2), \quad (10)$$

where the asterisk means complex conjugation, and the overbar symbolizes an average over an ensemble of field realizations. But Eq. (10) can also be written in the form

$$W(r_1, \theta_1, r_2, \theta_2) = \sum_{n,m} W_{nm}(r_1, \theta_1, r_2, \theta_2), \quad (11)$$

where

$$W_{nm} = \overline{E_n^*(r_1) E_m(r_2)} \exp(-in\theta_1) \exp(im\theta_2). \quad (12)$$

The terms of the series that appears in Eq. (11) can then be thought of as the cross-correlations between spiral modes, i.e., they provide, for $n \neq m$, the intermodal coherence features.

In this sense, after lengthy and careful calculations, it can be shown that matrices $\hat{M}^{(i)}$, $i = 0, 1, 2, 3$, can be expressed as follows

$$\hat{M}^{(0)} = \sum_n \hat{M}_m^{(0)}, \quad (13.a)$$

$$\hat{M}^{(1)} = \sum_n \hat{M}_{n-1n+1}^{(1)}, \quad (13.b)$$

$$\hat{M}^{(2)} = \sum_n \hat{M}_{n-1n+1}^{(2)}, \quad (13.c)$$

$$\hat{M}^{(3)} = \sum_n \hat{M}_m^{(3)}, \quad (13.d)$$

where

$$\hat{M}_m^{(0)} \Big]_{11} = \frac{2\pi}{I} \int_0^\infty r^2 \overline{|E_n|^2} r dr, \quad (14.a)$$

$$\hat{M}_m^{(0)} \Big]_{22} = \frac{2\pi}{k^2 I} \int_0^\infty \left(\overline{|E_n|^2} + \frac{n^2}{r^2} \overline{|E_n|^2} \right) r dr, \quad (14.b)$$

$$\hat{M}_m^{(0)} \Big]_{12} = \hat{M}_m^{(0)} \Big]_{21} = \frac{2\pi}{kI} \int_0^\infty r \operatorname{Im} \left\{ \overline{E_n} E_n^* \right\} r dr, \quad (14.c)$$

$$\hat{M}_{n-1n+1}^{(1)} \Big]_{11} = \frac{2\pi}{I} \int_0^\infty r^2 \operatorname{Re} \left\{ \overline{E_{n+1}} E_{n-1} \right\} r dr, \quad (14.d)$$

$$\begin{aligned} \hat{M}_{n-1n+1}^{(1)} \Big]_{22} &= \\ &= \frac{2\pi}{k^2 I} \int_0^\infty \text{Re} \left\{ \overline{(E'_{n+1})^* E'_{n-1}} - \frac{n^2-1}{r^2} \overline{E'_{n+1} E'_{n-1}} - \frac{n-1}{r} \overline{(E'_{n+1})^* E'_{n-1}} + \frac{n+1}{r} \overline{(E'_{n-1})^* E'_{n+1}} \right\} r dr, \end{aligned} \quad (14.e)$$

$$\hat{M}_{n-1n+1}^{(1)} \Big]_{12} = \hat{M}_{n-1n+1}^{(1)} \Big]_{21} = \frac{2\pi}{kI} \int_0^\infty r \text{Im} \left\{ \overline{E'_{n+1} E'_{n-1}} + \frac{n+1}{r} \overline{E'_{n+1} E'_{n-1}} \right\} r dr, \quad (14.f)$$

$$\hat{M}_{n-1n+1}^{(2)} \Big]_{11} = \frac{2\pi}{I} \int_0^\infty r^2 \text{Im} \left\{ \overline{E'_{n+1} E'_{n-1}} \right\} r dr, \quad (14.g)$$

$$\begin{aligned} \hat{M}_{n-1n+1}^{(2)} \Big]_{22} &= \\ &= \frac{2\pi}{k^2 I} \int_0^\infty \text{Im} \left\{ \overline{(E'_{n+1})^* E'_{n-1}} - \frac{n^2-1}{r^2} \overline{E'_{n+1} E'_{n-1}} - \frac{n-1}{r} \overline{(E'_{n+1})^* E'_{n-1}} - \frac{n+1}{r} \overline{(E'_{n-1})^* E'_{n+1}} \right\} r dr, \end{aligned} \quad (14.h)$$

$$\hat{M}_{n-1n+1}^{(2)} \Big]_{12} = \hat{M}_{n-1n+1}^{(2)} \Big]_{21} = \frac{2\pi}{kI} \int_0^\infty r \text{Re} \left\{ \overline{(E'_{n+1})^* E'_{n-1}} + \frac{n+1}{r} \overline{E'_{n+1} E'_{n-1}} \right\} r dr, \quad (14.i)$$

$$\hat{M}_{nn}^{(3)} \Big]_{11} = \hat{M}_{nn}^{(3)} \Big]_{22} = 0, \quad (14.j)$$

$$\hat{M}_{nn}^{(3)} \Big]_{12} = -\hat{M}_{nn}^{(3)} \Big]_{21} = \frac{2\pi}{kI} \int_0^\infty r \text{Re} \left\{ \frac{n}{r} \overline{|E_n|^2} \right\} r dr. \quad (14.k)$$

In these expressions, E_n was defined in Eq. (2), the prime indicates derivation with respect to r , and here $I = \int_0^{2\pi} \int_0^\infty W(r, \theta; r, \theta) r dr d\theta$.

As is apparent from Eqs. (13), the matrices $\hat{M}_{nn}^{(0)}$ and $\hat{M}_{nn}^{(3)}$ play a similar role as matrices $\hat{M}^{(0)}$ and $\hat{M}^{(3)}$ but now calculated for the functions W_{nn} , which can be understood as the CSD associated to each separate spiral mode. With regard to matrices $\hat{M}_{n-1n+1}^{(1)}$ and $\hat{M}_{n-1n+1}^{(2)}$, they exhibit an analogous structure to $\hat{M}^{(1)}$ and $\hat{M}^{(2)}$, but their elements are now computed from the functions W_{n-1n+1} (see Eq. (12)), which involve intermodal cross-correlations.

Taking all this into account, a number of direct consequences follow for general partially coherent beams:

- i) The focusing properties in the near- and far-field (beam width, divergence and waist-plane position, given by the elements of $\hat{M}^{(0)}$) do not depend on the intermodal coherence.
- ii) Accordingly, the beam quality parameter is also independent of any cross-correlation between spiral modes that constitutes the field.
- iii) The intermodal coherence has no influence on the z -component of the orbital angular momentum, J_z . In other words, different cross-correlation between spiral modes can give rise to the same value of J_z .
- iv) The orientation of the profile of a freely-propagating beam and the asymmetrical OAM, $J_z^{(a)}$ (both contained in matrices $\hat{M}^{(1)}$ and $\hat{M}^{(2)}$) depend on the cross-correlation between pairs of spiral modes separated by two orders ($n+1$ and $n-1$). When such a cross-correlation does not exist, the spatial profile does not rotate upon

free propagation, even though the rest of intermodal correlations differ from zero. In addition, $J_z^{(a)} = 0$.

- v) The vortex part, $J_z^{(v)}$, of the OAM also depends of the intermodal coherence of the pair of modes $n-1, n+1$. Property iii indicates, however, that such cross-correlation has no influence on the sum $J_z^{(a)} + J_z^{(v)} = J_z$.

4. Example

To illustrate the above general conclusions, let us now consider a light field represented by the following stochastic process at some transverse plane:

$$E(r, \theta) = f(r) \exp(i\theta) [\alpha \exp(-i\theta) + \beta \exp(i\theta)], \quad (15)$$

where $f(r)$ is real, and α and β denote random variables. Equation (15) means that the field $E(r, \theta)$ should be considered as a superposition of the two spiral modes $n-1$ and $n+1$ in the expansion (1). We have chosen this example because it allows illustrating the behavior in the general case. As a matter of fact, this field contains two spiral modes, separated by two orders. This enables us to handle, in a simple way, the intermodal coherence features (ranging from incoherence to complete coherence) through the random variables α and β . In addition, the spatial profile of the beam can be shaped by fixing a particular function $f(r)$.

For the above field, the irradiance reads

$$I(r, \theta) = f^2(r) \left[\overline{\alpha^2} + \overline{\beta^2} + 2 \operatorname{Re} \left\{ \overline{\alpha\beta^*} \exp(-2i\theta) \right\} \right], \quad (16)$$

and we also have $\langle x \rangle = \langle y \rangle = \langle u \rangle = \langle v \rangle = 0$. Let us now choose a (transverse) coordinate system with respect to which $\operatorname{Im} \left\{ \overline{\alpha\beta^*} \right\} = 0$. Note that this choice can always be done. The irradiance then becomes

$$I(r, \theta) = f^2(r) \left(\overline{\alpha^2} + \overline{\beta^2} \right) (1 + \sigma \Psi \cos 2\theta), \quad (17)$$

where

$$\sigma = \frac{\overline{\alpha\beta^*}}{\left(\overline{\alpha^2} \overline{\beta^2} \right)^{1/2}}, \quad (18.a)$$

$$\Psi = \frac{2 \left(\overline{\alpha^2} \overline{\beta^2} \right)^{1/2}}{\overline{\alpha^2} + \overline{\beta^2}}. \quad (18.b)$$

It follows at once that

$$0 \leq |\sigma| \leq 1. \quad (19)$$

The value $|\sigma|=1$ implies a coherent superposition of the two spiral modes, whereas $\sigma=0$ means that the modes should be considered as incoherent (mutually uncorrelated). An intermediate value $0 < |\sigma| < 1$ would correspond to a partially coherent superposition.

On the other hand, it can be shown that

$$0 \leq \Psi \leq 1. \quad (20)$$

The factor Ψ depends on the relative weight of the spiral modes that contributes to the stochastic field. It reaches its maximum value $\Psi = 1$ when $\overline{\alpha^2} = \overline{\beta^2}$.

In the present example, the matrices $\hat{M}^{(i)}$, $i = 0, 1, 2, 3$, calculated at the transverse plane where the field is given by Eq. (15), take the form

$$\hat{M}^{(0)} = \begin{pmatrix} \langle r^2 \rangle & 0 \\ 0 & \xi + (1+n^2 + 2n \cos 2\gamma)\rho \end{pmatrix}, \quad (21.a)$$

$$\hat{M}^{(1)} = \frac{\sigma\Psi}{2} \begin{pmatrix} \langle r^2 \rangle & 0 \\ 0 & \xi + (1-n^2)\rho \end{pmatrix}, \quad (21.b)$$

$$\hat{M}^{(2)} = \frac{\sigma\Psi}{2} \begin{pmatrix} 0 & \frac{n}{k} \\ \frac{n}{k} & 0 \end{pmatrix}, \quad (21.c)$$

$$\hat{M}^{(3)} = \begin{pmatrix} 0 & \frac{1}{k}(n + \cos 2\gamma) \\ -\frac{1}{k}(n + \cos 2\gamma) & 0 \end{pmatrix}, \quad (21.d)$$

where

$$\langle r^2 \rangle = \frac{\int_0^\infty r^2 f^2(r) r dr}{\int_0^\infty f^2(r) r dr}, \quad (22.a)$$

$$\xi = \frac{1}{k^2} \frac{\int_0^\infty [f'(r)]^2 r dr}{\int_0^\infty f^2(r) r dr}, \quad (22.b)$$

$$\cos 2\gamma = \frac{\overline{\beta^2} - \overline{\alpha^2}}{\overline{\alpha^2} + \overline{\beta^2}}, \quad (22.c)$$

$$\rho = \frac{1}{k^2} \frac{\int_0^\infty \frac{f^2(r)}{r^2} r dr}{\int_0^\infty f^2(r) r dr}. \quad (22.d)$$

Taking the above expressions into account, we get the following overall spatial behavior:

i) Incoherent case ($\sigma = 0$)

- The beam is rotationally symmetric, and both the beam quality parameter and the specific value of the OAM depend on the relative weight of the spiral modes, for a given n .

- The asymmetrical OAM, $J_z^{(a)}$, vanishes. In other words, the OAM only involves the vortex part.

ii) Partially coherent case ($\sigma \neq 0$)

- The beam is not rotationally symmetric, and $J_z^{(a)}$ differs from zero. In fact,

$$J_z^{(a)} = \frac{I}{c} \left(\frac{n}{k} \frac{\sigma \Psi}{2} \right), \quad (23.a)$$

and

$$J_z = \frac{I}{c} \frac{1}{k} (n + \cos 2\gamma). \quad (23.b)$$

We see that $J_z^{(a)}$ is maximum when $\sigma = 1$ (coherent case) and $\Psi = 1$ (same weight of the spiral modes). Also note that $J_z^{(a)} = 0$ for $n = 0$.

- The spatial profile of this beam rotates upon free propagation, and its rotation is independent of σ and Ψ (it depends on n and $f(r)$). To characterize such rotation, we can apply Eq. (5).

Figures 1-3 illustrate the transverse structure of the irradiance profile $I(r, \theta)$ for the special case

$$f(r) = \left(\frac{r}{w} \right)^{n+1} \exp\left(-\frac{r^2}{2w^2}\right). \quad (24)$$

In accordance with the analytical results, we see from the figures that the beam shape exhibits a rotationally-symmetric structure when the spiral modes are uncorrelated ($\sigma = 0$). Otherwise, the profile shows the appearance of two lobes, which becomes more pronounced for higher values of the product $\sigma\Psi$.

Finally, Fig. 4 shows the rotation of the beam profile in terms of the propagation distance z , for several values of n . In this case, the evolution of the angle α , given by Eq. (5), reduces to the formula

$$\tan 2\alpha(z) = \frac{2nz}{kw^2(n+2) + \frac{z^2}{kw^2}(2-n)}. \quad (25)$$

Note first that, for $n = 0$, the irradiance profile does not rotate, as it should be expected. In addition, a nearly asymptotic behavior of the curves plotted in Fig. 4 is observed for distances longer than, say, 30 cm from the initial plane. Note also that the numerical value $kw^2/2$ would be the Rayleigh length associated to a coherent Gaussian beam, w being the beam width at its waist plane. For the values chosen in Fig. 4, $kw^2/2 \approx 1.6\text{cm}$. It should be remarked, however, that, for partially coherent light, the Rayleigh length z_R associated to the set of beams defined by Eq. (24) depends on n as well as on the relative weight between modes, and the resulting expression for z_R would become more involved.

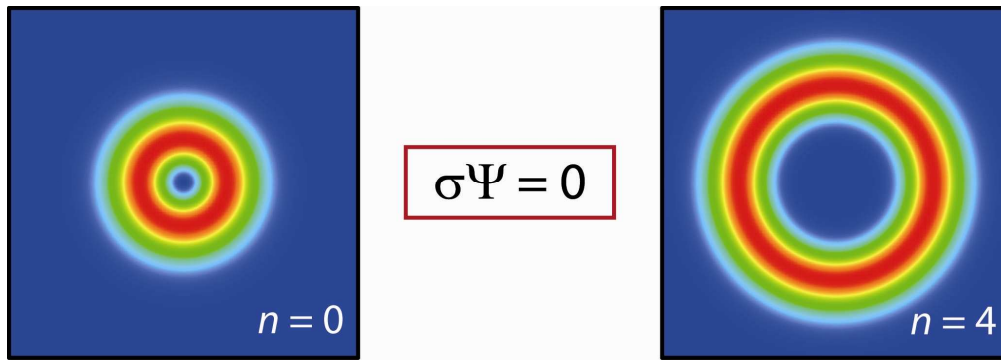


Fig. 1. Transverse distribution (pseudo-coloured) proportional to the irradiance profile of the field considered in the example analysed in Section 4 (cf. Equations (17) and (24)), for the values $w = 100\lambda$, $\lambda = 0.5 \mu\text{m}$, $\sigma\Psi = 0$. As usual, the horizontal and vertical directions correspond to the x- and y-axis, respectively. The length of the side of each square is $4w$.

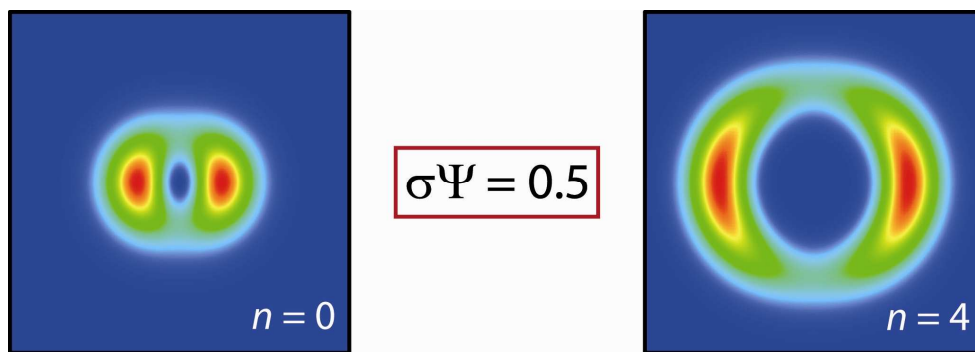


Fig. 2. The same as in Fig. 1 but now with $\sigma\Psi = 0.5$.

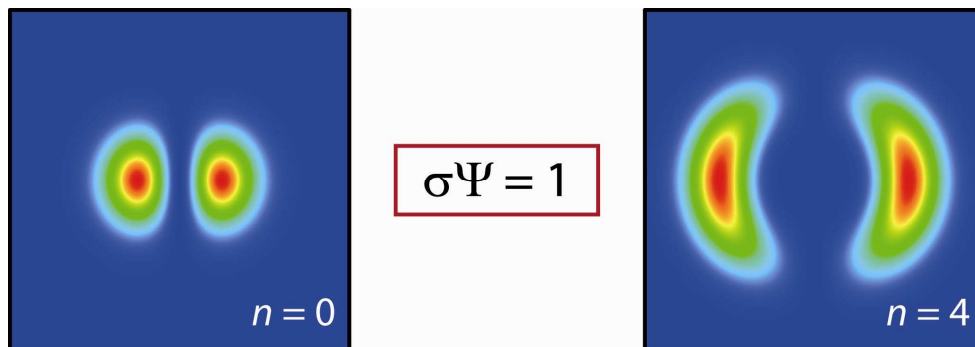


Fig. 3. The same as in Fig. 1 but now with $\sigma\Psi = 1$.

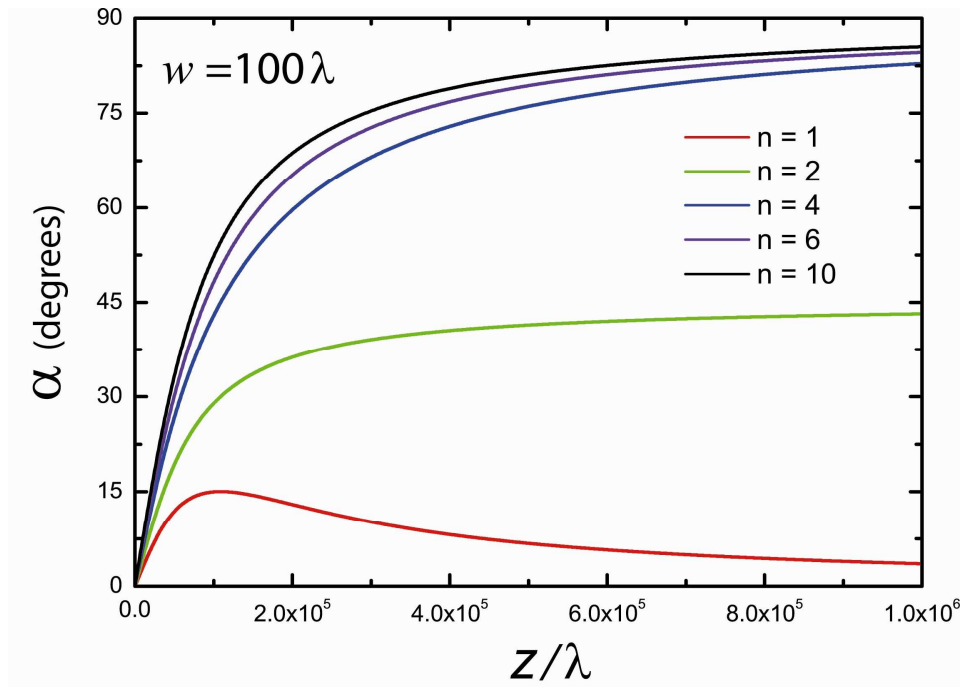


Fig. 4. Rotation angle α of the beam profile upon free propagation, for the example considered in Section 4.

5. Conclusions

The so-called spiral modes associated to a partially coherent beam can be understood as the terms of the spiral-harmonics expansion of the field. It is then meaningful to write the CSD as a series whose terms provide the cross-correlations between spiral modes (in short, their intermodal coherence features). Several relations have been derived between certain spiral-content characteristics and the spatial beam structure. In particular, it has been concluded that the OAM, J_z , the beam quality parameter and the focusing properties at the near- and far-field do not depend on the intermodal coherence. On the contrary, the orientation of the beam profile and both the asymmetrical and the vortex parts, $J_z^{(a)}$ and $J_z^{(v)}$, of the OAM depend on the cross-correlation between pair of modes separated by two orders, namely, $n + 1$ and $n-1$.

Acknowledgements

This work has been supported by the Ministerio de Educación y Ciencia of Spain, project FIS2007-63396.